

H I ABSORPTION TOWARD THE NUCLEUS OF THE POWERFUL RADIO GALAXY CYGNUS A: EVIDENCE FOR AN ATOMIC OBSCURING TORUS?

J. E. CONWAY¹

National Radio Astronomy Observatory, P.O. Box 0, Socorro, NM 87801

AND

P. R. BLANCO

Center for Astrophysics & Space Sciences, University of California, San Diego, 9500 Gilman Drive, La Jolla, CA 92093-0111

Received 1995 March 9; accepted 1995 June 14

ABSTRACT

We report the detection of broad (FWHM 270 km s^{-1}) H I $\cdot 21 \text{ cm}$ absorption toward the compact ($<15 h^{-1} \text{ pc}$) radio nucleus of the nearby powerful radio galaxy Cygnus A. The absorption corresponds to a column density of hydrogen atoms of at least $2.54 \pm 0.44 \times 10^{19} T_{\text{spin}} \text{ cm}^{-2}$. Observations of OH and H₂CO yielded upper limits. While other possibilities exist, we argue that the observed H I absorption plausibly occurs within a circumnuclear obscuring torus which is thought to block our direct view of a quasar nucleus in this object.

We have attempted to constrain the properties of the obscuring gas by combining our H I result with upper limits on molecular absorption and estimates of the total obscuring column density from X-ray observations. One possibility is that the majority of the gas is in a hot ($\approx 8000 \text{ K}$) mainly atomic phase; we derive limits on the size of such an atomic torus. Alternatively, the H I absorption might be caused by atomic gas within a warm ($\approx 1000 \text{ K}$) mainly molecular torus. In this case, the nondetection of molecular absorption can possibly be explained by radiative excitation due to the central radio source.

Follow-up VLBI observations are planned which will further constrain the properties of the absorbing gas and distinguish between the competing models.

Subject headings: galaxies: active — galaxies: individual (Cygnus A) — galaxies: nuclei — radio lines: galaxies — radio lines: ISM

1. INTRODUCTION

In the strongest form of the quasar/radio galaxy unified scheme it is proposed that all powerful radio-loud objects contain a quasar nucleus, and that narrow-line radio galaxies are those objects oriented such that a dense obscuring torus blocks our direct view of this nucleus (Barthel 1989). As the nearest powerful FR II radio galaxy ($z = 0.0565$), Cygnus A has recently been the subject of a number of studies which test the predictions of this unified scheme. Several lines of evidence now suggest that Cyg A does indeed harbor a quasar nucleus, hidden from direct view in the visible and soft X-rays by a dusty obscuring torus (e.g., Ward et al. 1991; Antonucci, Hurt, & Kinney 1994). Furthermore, X-ray spectroscopy by the *Ginga* satellite (Ueno et al. 1994) has confirmed the presence of a highly absorbed hard X-ray source, with an intrinsic 2–10 keV luminosity of $2.5 \times 10^{44} h^{-2} \text{ ergs s}^{-1}$ ($h = H_0/100$) and an equivalent foreground column density $N_{\text{H}} = 3.75 \pm 0.73 \times 10^{23} \text{ cm}^{-2}$ (90% errors), consistent with the notion of a buried quasar in Cyg A.

In this paper we describe Very Large Array (VLA)² observations in search of spectral absorption by the species H I, OH, and H₂CO (formaldehyde) toward the compact radio nucleus of Cyg A (of size $<15 h^{-1} \text{ pc}$; Carilli, Bartel, & Linfield 1991, Carilli, Bartel, & Diamond 1994). Our objectives were to search for direct evidence of neutral obscuring gas, and by

combining our results with observations in other wave bands, to constrain the location and physical state of this gas.

2. OBSERVATIONS AND DATA REDUCTION

Details of the VLA observations are given in Table 1. In the initial A-array observations, two slightly overlapping IFs were observed at each transition in order to improve the velocity sampling. In the follow-up B-array observations (at H I only), a single IF band was observed. All observations used on-line Hanning smoothing.

Data reduction proceeded by (i) interactively editing to remove the sporadic effects of radio interference, (ii) amplitude- and phase-calibrating the data, (iii) making continuum images by averaging together several frequency channels, and then iteratively deconvolving and self-calibrating. Since no sufficiently bright calibrator exists, bandpass solutions were obtained from the Cyg A data themselves, using only short baselines with continuum flux densities $>70 \text{ Jy}$ for H I and OH ($>10 \text{ Jy}$ for H₂CO). Since these short baselines were dominated by lobe emission, and not emission from the 0.8 Jy core, this procedure is valid provided there is no spectral emission or absorption from the lobes—a possibility checked by applying the solutions obtained to calibrator data (see § 3). Finally, continuum emission was removed from the data using a combination of the AIPS tasks UVSUB and UVLIN, the data were Fourier inverted, and spectra were plotted at the core position.

3. RESULTS

H I absorption toward the nucleus of Cyg A was detected in the original A-array data and confirmed in the follow-up

¹ Present address: Onsala Space Observatory, Onsala, S-43992, Sweden.

² The VLA is a facility of the National Radio Astronomy Observatory, which is operated by Associated Universities Inc., under cooperative agreement with the National Science Foundation.

TABLE 1
LOG OF THE VLA OBSERVATIONS

Species and Rest Frequency (MHz)	Array Configuration	UT Date	Center Frequency (MHz)	Duration (minutes)	Spectral Sampling (km s ⁻¹)	Velocity Coverage (km s ⁻¹)
H I (1420)	A	1994 Mar 11	1344	55	11.5	1010
OH (1667).....	A	1994 Mar 11	1579	55	8.3	730
H ₂ CO (4830).....	A	1994 Mar 11	4571	55	54.0	1190
H I (1420).....	B	1994 July 4	1344	20	23.0	1100

B-array observations (see Fig. 1). At positions away from the core, the measured rms noise per spectral channel in each spectrum (9 mJy per beam and 11 mJy per beam, respectively) is close to that expected theoretically, though the residuals in the B-array data cube showed slight systematic artifacts (ripples), perhaps as a result of residual radio interference effects or the sparse uv coverage. Within the noise, however, the A- and B-array spectra are identical.

To quantify the size of any residual bandpass effects in the H I data, we applied the bandpass solutions derived using the short baselines on Cyg A (see § 2) to our point source calibrator (BL Lacertae). The resulting calibrator spectra only show thermal noise; in the case of the A-array observations, the spectral dynamic range (continuum flux density divided by rms noise per channel) is $>500:1$; we can then be certain that residual bandpass effects are much less than the observed absorption toward the Cyg A nucleus. This procedure also rules out any significant H I absorption against the lobes of Cyg A (Lilley & McClain 1956); such absorption would show up as apparent H I emission toward the calibrator source.

The best-fitting single Gaussian models for the A- and B-array data require $\text{FWHM} = 276 \pm 26 \text{ km s}^{-1}$ and $379 \pm 62 \text{ km s}^{-1}$, respectively (we use 1σ uncertainties throughout). However, the A-array spectrum shows strong evidence that the absorption is split into two components; a two-Gaussian fit yields centroid velocities of $+40 \pm 6$ and $-149 \pm 8 \text{ km s}^{-1}$ for these components, with $\text{FWHM} = 151 \pm 16 \text{ km s}^{-1}$ and $102 \pm 20 \text{ km s}^{-1}$, respectively. Based on the reduced χ^2 (83.7/81 dof), this two-Gaussian fit to the A-array spectrum is highly favored over the single Gaussian model (124.1/84 dof).

Independent of the model, we find that the integrated absorption from -400 to $+200 \text{ km s}^{-1}$ is -10.60 ± 0.75 and $-10.75 \pm 1.29 \text{ Jy km s}^{-1}$ for the A- and B-array spectrum, respectively.

The corresponding H I column density depends on the flux density of the VLA core and what fraction of this core (which is resolved on parsec scales) is covered by the absorbing H I screen. We estimate that the flux density of the unresolved VLA core is $778 \pm 128 \text{ mJy}$ (the large uncertainty is related to the lack of short baselines in the A-array observations and the poor B-array uv coverage). Although there are no VLBI continuum images at 1.4 or 1.6 GHz, in the 5 GHz VLBI map presented by Carilli et al. (1994) almost all the VLA core flux density occurs within a jet $15 h^{-1} \text{ pc}$ long. Beyond this distance, the jet surface brightness rapidly falls off, and so it is probable that most of the flux density at 1.34 GHz occurs within a similar scale. It follows that if the absorbing screen has size $>15 h^{-1} \text{ pc}$, then all the continuum emission is covered and the observed H I absorption implies an H I column of $2.54 \pm 0.44 \times 10^{19} T_{\text{spin}} \text{ cm}^{-2}$, where T_{spin} is the spin temperature; if the screen is smaller, then the column must be larger.

Our OH and H₂CO observations show no evidence for significant absorption or emission. The OH observations, which were somewhat effected by radio interference (see § 2) generally had a noise per channel only slightly larger than thermal, i.e., 12 mJy beam⁻¹ (though several channels had an rms noise of 18 mJy beam⁻¹). The corresponding 3σ limit on the opacity of OH absorption of FWHM Δv is $1.3 \times 10^{-2} (\Delta v/100 \text{ km s}^{-1})^{-1/2}$ (assuming a continuum core flux density of 0.8 Jy). The core spectra for formaldehyde showed features

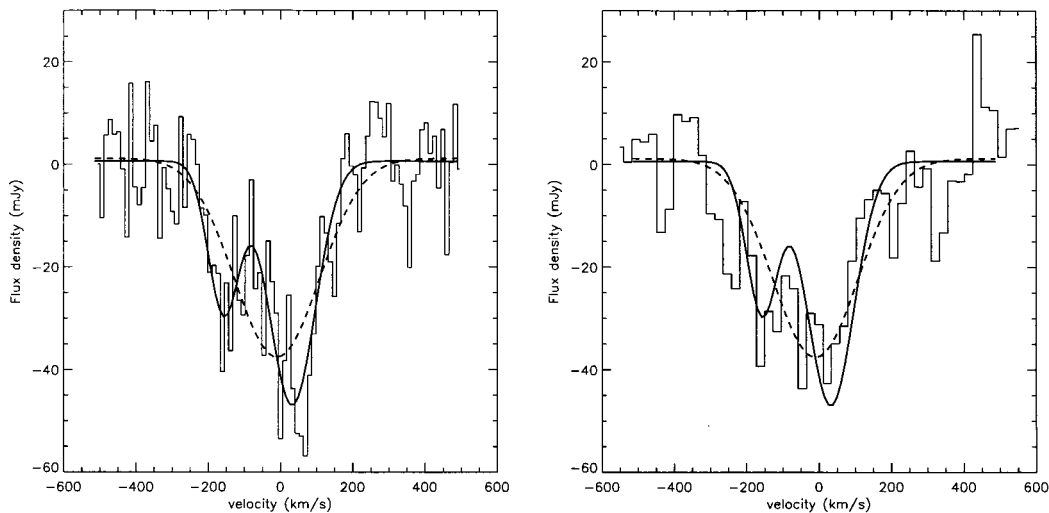


FIG. 1.—VLA spectra of the core of Cyg A (see § 2). *Left*, A-array: spectral sampling is 11.5 km s^{-1} , synthesized beam $1.3''$; *Right*, B-array: spectral sampling is 23 km s^{-1} , synthesized beam $4.3''$. The best-fitting one- and two-Gaussian models to the A-array data are shown as dashed and solid lines, respectively. Channel velocities v are calculated from $v = (1420405.7/\nu - 1.0565) \times c$, where ν is the observed frequency (in Hz) corrected to the heliocentric reference frame.

above the thermal noise, but these are probably a result of residual bandpass or continuum subtraction effects; from the highest channel residual (8 mJy), we obtain an opacity limit in H_2CO of ≈ 0.01 per 54 km s^{-1} resolution element.

4. DISCUSSION

4.1. The Location of the H I Obscuring Gas

First we consider whether the observed H I absorption could arise in a kiloparsec-scale dust lane. Measurements of the Paschen and Balmer lines imply (after taking into account the extinction in our Galaxy) a foreground extinction of $A_V = 1.2$ mag toward the narrow-line region (Ward et al. 1991). For a normal dust-to-gas ratio, the associated gas column could easily account for the integrated H I opacity. The required gas spin temperature would be 100 K for a wholly atomic column but less if the column were partly molecular.

However, a serious problem with this interpretation is the large velocity width of the absorption (FWHM = 270 km s^{-1}). In known cases of dust lane ellipticals with associated H I absorption, this absorption occurs within multiple narrow components, which is quite different to what we see in Cyg A (van Gorkom et al. 1986, 1989; van der Hulst, Golisch, & Haschick 1983; Dwarakanath, Owen, & van Gorkom 1995). Conversely, in those objects, which like Cyg A, have broader ($>150 \text{ km s}^{-1}$) H I absorption profiles, there is increasing evidence that the absorption occurs close to the nucleus (NGC 4151: $r < 50 \text{ pc}$, Mundell et al. 1995; NGC 4261: $r \approx 100 \text{ pc}$, Jaffe & McNamara 1994).

Broad velocity widths for circumnuclear tori are also consistent with theoretical predictions (Krolik & Begelman 1988) because in order for tori to be geometrically thick, the cloud dispersion velocity within the torus must approximately equal the orbital velocity, i.e., typically a few hundred km s^{-1} . Torus models can also give a natural explanation of the apparently split line seen in Cyg A (see § 3) if the torus gas rotates around a parsec-scale radio jet which is somewhat edge-brightened and oriented close to the sky plane. Gas seen in absorption against one edge of the jet would then be slightly redshifted, and blueshifted against the other. If the torus were not much larger than the jet width, the two velocity components would be separated by roughly the orbital velocity. This hypothesis will be tested by upcoming H I VLBI observations. In Cyg A, both the line splitting and component widths are roughly 150 km s^{-1} ; taking this as an indication of the orbital velocity, we find that this would correspond to gas in orbit at $\sim 10 \text{ pc}$ from a black hole of $\sim 10^8 M_\odot$, which at 10% of its Eddington luminosity could provide the observed X-ray to far-infrared luminosity of $\sim 10^{45} h^{-2} \text{ ergs s}^{-1}$.

Physical models of circumnuclear tori have been investigated by Krolik & Lepp (1989), Maloney, Begelman, & Rees (1994), Neufeld, Maloney, & Conger (1995), and Maloney, Hollenbach, & Tielens (1995). An important result is that the circumnuclear material can be either atomic or molecular depending on the value of the effective ionization parameter $\xi_{\text{eff}} = 4\pi F_X N_{22}^{-0.9}/n = L_X N_{22}^{-0.9}/nr^2$ (Maloney et al. 1994), where L_X and F_X are the luminosity and local flux density of $>2 \text{ keV}$ X-rays, n is the local gas density, r is the distance to the nucleus, N_{22} is the total column density in units of 10^{22} cm^{-2} , and the factor $N_{22}^{-0.9}$ takes into account the effects of photoelectric absorption. If $\xi_{\text{eff}} > 10^{-3}$ (in Maloney et al.'s units), the gas must be largely atomic, otherwise it is mainly molecular; we discuss these two possibilities below in §§ 4.2 and 4.3.

4.2. An Atomic Obscuring Torus

Support for a largely atomic obscuring column in Cyg A comes from the absence of detectable CO (Barvainis & Antonucci 1994), NH_3 (Barvainis 1995), OH, or formaldehyde absorption (see § 3). Although other explanations are possible (see § 4.3), the simplest is that this absorption does not occur because most of the gas along the line of sight is atomic. Maloney et al. (1994) find that an atomic torus results if $\xi_{\text{eff}} > 0.001$; using the hard X-ray luminosity reported by Ueno et al. (1994), this implies that the torus will be largely atomic provided that its outer radius $r_{\text{outer}} < 32 h^{-1} n_6^{-1/2} \text{ pc}$, where n_6 is the H I number density in the torus clouds in units of 10^6 cm^{-3} .

A purely atomic torus can quite naturally account for the magnitude of both the observed H I integrated opacity and the total column density inferred from X-ray observations. If the torus is large enough to cover most of the compact radio jet at 1.34 GHz (i.e., has outer radius $>15 h^{-1} \text{ pc}$), then the observed H I opacity requires a column density of H I of $2.54 \pm 0.44 \times 10^{19} T_{\text{spin}} \text{ cm}^{-2}$ (see § 3). Atomic gas irradiated by hard X-rays is predicted to have a stable equilibrium state at a temperature of $\approx 8000 \text{ K}$, almost independent of density (Lepp et al. 1985; Neufeld et al. 1995). It can be shown that the increase in line-of-sight-averaged spin temperature owing to radiative excitation effects (Bahcall & Ekers 1969) will be less than a factor of 2 provided that $r_{\text{outer}} > 4.4 n_6^{-1/2} \text{ pc}$, where r_{outer} , the torus outer radius, is assumed to be much larger than the inner radius. Assuming a spin temperature in the range 8000–16000 K, the required H I column density to give our observed H I absorption is then in the range $2.0\text{--}4.0 \times 10^{23} \text{ cm}^{-2}$, in excellent agreement with the total column density derived from X-ray observations (§ 1).

Since an atomic torus contains a significant fraction of free electrons (i.e., 0.01; Neufeld et al. 1995), there is an additional constraint on torus properties owing to the lack of observable free-free absorption effects. The fact that the observed VLA core spectrum is flat (in F_ν) down to at least 1.34 GHz suggests that the free-free opacity at 1.34 GHz is less than about 0.5. Assuming electron fractions of 0.01, electron temperatures of 8000 K, and a total column density $N_{\text{H}} = 3.7 \times 10^{23} \text{ cm}^{-2}$ (Ueno et al. 1994), this implies gas densities $n < 2 \times 10^5 \text{ cm}^{-3}$. Substituting this density limit into the radiative excitation limit discussed above, we find that an atomic torus of radius 15 pc or greater is able to satisfy the radiative excitation and free-free constraints simultaneously.

In contrast, a smaller atomic torus would have difficulty fitting all the constraints. Such a torus would only cover part of the continuum structure, increasing the column densities required to explain the observed H I absorption (see § 3). Furthermore, the high densities within such a torus would increase the effects of free-free absorption, while the proximity to the nucleus would increase radiative excitation.

While a detailed analysis is not possible until maps are made of the 1.34 GHz parsec-scale continuum emission (and is complicated by the uncertainty in H_0 and the large errors on N_{H}), it appears the above arguments already rule out a very compact torus with $r_{\text{outer}} < 5 \text{ pc}$ which only covers the ‘‘core’’ component visible in the 5 GHz VLBI maps of Carilli et al. (1994). From numerical simulations of radiative transfer through such a torus, we find that there is a minimum intrinsic 1.34 GHz core flux density of 1.76 Jy (and an associated column density $1.6 \times 10^{24} \text{ cm}^{-2}$) which admits solutions for the

observed H I opacity (giving an apparent 1.34 GHz flux density of 480 mJy after taking into account free-free effects). This minimum flux density arises because if we try to duplicate the observed H I absorption using a lower core flux and larger H I column density, we find that the associated free electrons completely absorb the background continuum source, such that we cannot achieve the observed line depth. In contradiction to this theoretical minimum, we estimate a 1.34 GHz core flux density of less than 100 mJy (λ by extrapolating the 5 GHz flux density of 300 mJy using the estimated 43 – 5 GHz spectral index $\alpha > 0.9$ where $F_\nu \propto \nu^\alpha$; Carilli et al. 1994). The only way the core can be bright enough at 1.34 GHz, without overpredicting the total flux density visible in our VLA map, is for the VLBI core spectrum to have a sharp minimum near 5 GHz while the parsec-scale *jet* spectrum is flat or rising between 1.34 GHz and 5 GHz. Both properties would be highly unusual compared to typical VLBI jets (see Marscher 1988).

We note in passing that despite the high temperatures predicted for atomic tori (≈ 8000 K), this gas could still contain enough dust to explain the derived optical/IR obscuration of $A_V = 50$ –100 mag (Ward et al. 1991; Djorgovski et al. 1991). Since the grain temperature is set by the effective temperature of the local radiation field (Neufeld et al. 1995), its temperature can be much less than the gas. Given the hard X-ray luminosity derived for Cyg A (Ueno et al. 1994), from Neufeld et al. (1995) we find that grain temperatures in Cyg A should only exceed sublimation temperature of ≈ 1000 K within a radius $0.4 h^{-1/2}$ pc.

4.3. A Molecular Obscuring Torus

It is still possible that the majority of the obscuring column toward Cyg A is in a molecular state. Various explanations (see below) are possible for the lack of detectable molecular absorption (in any of the species CO, OH, H₂CO, or NH₃). Such models are certainly consistent with the observed H I opacity. The models of Krolik & Lepp (1989) predict clouds with temperatures of order 1000 K, and depending on conditions a wide range of H I fractions from 0.05 to about 0.5. If the torus is large ($> 15 h^{-1}$ pc) and covers the whole VLBI radio jet, then adopting $T_{\text{spin}} = 1000$ K, the required $N_{\text{H I}}$ is $\approx 2.5 \times 10^{22} \text{ cm}^{-2}$, which is consistent with the total column density given by Ueno et al. (1994) if the H I abundance is 0.07. Conversely, if the torus is small ($< 5 h^{-1}$ pc) and just covers the radio core, which is predicted to have flux density of ≈ 100 mJy at 1.34 GHz (see § 4.2), then the required H I abundance is 0.5. While these calculations assume no radiative excitation of the H I, this can easily be realized even in the compact torus case, by having low cloud filling factors and high cloud densities. In

contrast to a hot, atomic torus (see § 4.2), there are no constraints resulting from free-free absorption because the free electron fraction is negligible (Neufeld et al. 1995).

As noted by Barvainis & Antonucci (1994), CO($J = 1-0$) absorption might have escaped detection if the molecular clouds are smaller than the background source and have a covering factor of about unity (as expected) and a large velocity dispersion. If the clouds were hot ($T \approx 1000$ K) and were distributed over a velocity range similar to that of the detected H I absorption, they would indeed be below the detection level of the Barvainis & Antonucci observations; a more sensitive search is clearly required. The other possible explanation for the nondetection of CO is radiative excitation via millimeter-wave continuum emission from the nucleus (Maloney et al. 1994). Note that it is quite possible for the cloud density to be such that CO is radiatively excited but H I is not. Assuming a flat spectrum continuum source, then at any given distance/CO radiative excitation is still significant at densities 30 times larger than those for which it ceases to be important for H I (Bahcall & Ekers 1969).

Given the abundances of OH predicted in some molecular torus models (e.g., Krolik & Lepp 1989), our nondetection of OH absorption is hard to explain unless this too is radiatively excited. Assuming the OH absorbing gas has a similar velocity dispersion and temperature to the H I, then if there is no radiative excitation the expected ratio of OH to H I opacity $\tau_{\text{OH}}/\tau_{\text{H I}} = 8.2 \times 10^3 x_{\text{OH}}/x_{\text{H I}}$, where x_{OH} and $x_{\text{H I}}$ are the fractional abundances of OH and H I, respectively. For the wide variety of torus models investigated by Krolik & Lepp (1989) the minimum value of $x_{\text{OH}}/x_{\text{H I}}$ is 1.2×10^{-4} , implying $\tau_{\text{OH}}/\tau_{\text{H I}} > 1$ compared to the observed upper limit (see § 3) of 0.08. However, more recent modeling (Neufeld et al. 1995; Maloney et al. 1995) predicts that at least in high pressure ($10^{11} \text{ K cm}^{-3}$) warm (500–1000 K) molecular tori, OH is efficiently converted to H₂O; this is one possible explanation for the lack of detectable OH absorption. Alternatively, OH might be radiatively excited; unfortunately, published calculations for OH and other molecules (e.g., Rogers & Barrett 1968) do not deal with the pressures and temperatures expected in circumnuclear tori; more work is required in this area to understand the implications of our nondetection of OH absorption.

We are grateful to Michael Rupen, Elias Brinks, and Phil Maloney for useful discussions, and to Alan Pedlar for initially suggesting this work. J. E. C. acknowledges the support of an NRAO Jansky Fellowship and a JIVE fellowship. P. R. B. was supported in part by an SERC fellowship, and in part by NASA contract NAS 5-30720.

REFERENCES

- Antonucci, R. A., Hurt, T., & Kinney, A. 1994, *Nature*, 371, 313
 Bahcall, J. N., & Ekers, R. D. 1969, *ApJ*, 157, 1055
 Barthel, P. D. 1989, *ApJ*, 336, 606
 Barvainis, R. 1995, in *Proc. Cygnus A Workshop*, ed. D. Harris & C. Carilli (Cambridge: Cambridge Univ. Press), in press
 Barvainis, R., & Antonucci, R. A. 1994, *AJ*, 107, 1291
 Carilli, C. L., Bartel, N., & Diamond, P. J. 1994, *AJ*, 108, 64
 Carilli, C. L., Bartel, N., & Linfield, R. P. 1991, *AJ*, 102, 1691
 Djorgovski, S., Weir, N., Matthews, K., & Graham, J. R. 1991, *ApJ*, 372, L67
 Dwarakanath, K. S., Owen, F. N., & van Gorkom, J. H. 1995, *ApJ*, 442, L1
 Jaffe, W., & McNamara, B. R. 1994, *ApJ*, 434, 110
 Krolik, J. H., & Begelman, M. C. 1988, *ApJ*, 329, 702
 Krolik, J. H., & Lepp, S. 1989, *ApJ*, 347, 179
 Lepp, S., McCray, R., Shull, J. M., Woods, D. T., & Kallman, T. 1985, *ApJ*, 288, 58
 Lilley, A. E., & McClain, E. F. 1956, *ApJ*, 123, 172
 Marscher, A. P. 1988, *ApJ*, 334, 552
 Maloney, P. R., Begelman, M. C., & Rees, M. J. 1994, *ApJ*, 432, 606
 Maloney, P. R., Hollenbach, D. J., & Tielens, A. G. G. M., 1995, in preparation
 Mundell, C. G., Pedlar, A., Baum, S. A., O’Dea, C. P., Gallimore, G. F., & Brinks, E. 1995, *MNRAS*, 272, 355
 Neufeld, D. A., Maloney, P. R., & Conger, S. 1995, *ApJ*, 436, L127
 Rogers, A. E. E., & Barrett, A. H. 1968, *ApJ*, 151, 163
 Ueno, S., Koyama, K., Nishida, M., Yamauchi, S., & Ward, M. J. 1994, *ApJ*, 431, L1
 van der Hulst, J. M., Golisch, W. F., & Haschick, A. D. 1983, *ApJ*, 264, L37
 van Gorkom, J. H., Knapp, G. R., Ekers, R. D., Ekers, D. D., Laing, R. A., & Polk, K. S. 1989, *AJ*, 97, 708
 van Gorkom, J. H., Knapp, G. R., Raimond, E., Faber, S. M., & Gallagher, J. S. 1986, *AJ*, 91, 791
 Ward, M. J., Blanco, P. R., Wilson, A. S., & Nishida, M. 1991, *ApJ*, 382, 115